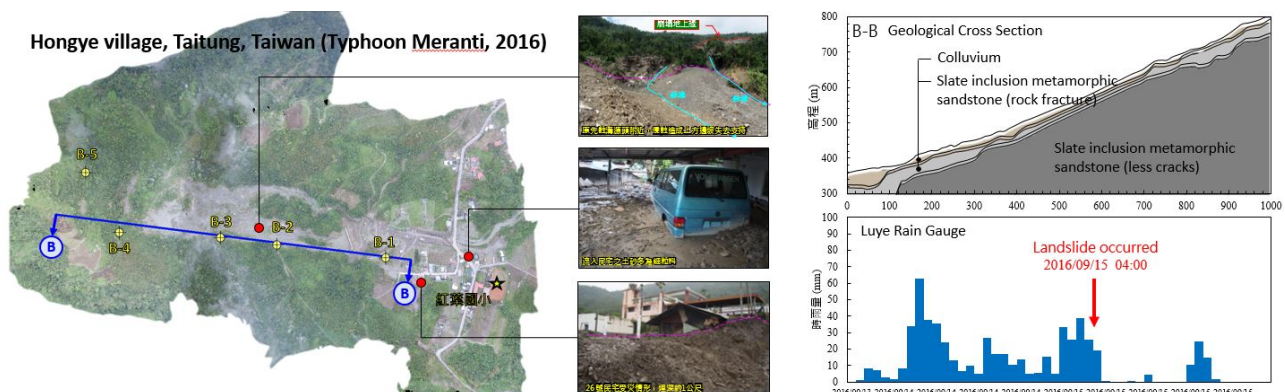


## Simulation of Large-Scale Shallow Landslide Triggered by Heavy Rainfall using IRIS Model

○Chen-Yu Chen (陳振宇), Hsuan-Pin Wu(吳軒蘋), Jyun-Wei Chen(陳均維), Kuo-Wei Chen(陳國威)  
Soil and Water Conservation Bureau, Taiwan (台灣水土保持局)

### 1. INTRODUCTION

A large-scale landslide at Hongye village, Taitung, Taiwan was triggered by typhoon Meranti, causing accumulated rainfall of over 500mm within 24 hours in 2016 (**Fig. 1**). To obtain overall impact area of post disaster, the unmanned aerial vehicle (UAV) was used for survey. In addition, an integrated rain-fall-infiltration-slope stability model (IRIS model), which was developed by Tsutsumi (2008), was selected to simulate Hongye landslide. IRIS model is divided into three stages. Firstly, the variation of water content is described by Richard's equation, performing finite-element method to solve the process of rainfall-infiltration. Secondly, the concept of limit equilibrium using Janbu's simplified method is utilized for slope stability analysis. Afterward, the critical slip surface is determined by dynamic programming method. The soil physical and engineering properties were investigated from in-situ sampling and laboratory test by Soil Water Conservation Bureau. The results indicate that landslide occurrence time and failure slip surface can be effectively simulated by IRIS model.



**Fig. 1** A large-scale landslide disaster at Hongye village, Taitung, Taiwan during typhoon Meranti in 2016.

### 2. METHOD

#### (1) Post Disaster Survey and Assessment

To investigate the disaster situation, UAV was employed to build the 3D model, orthophoto and digital surface model (DSM). This study uses remote-controlled UAV Phantom 3 Professional equipped with digital camera and GPS to acquire airborne digital photographs on September 16, 2016 and March 24, 2017. The images recorded in 2016 is in emergency mission, the image resolution ranges between 0.042m to 0.370m, and did not set the ground control point. UAV mission in 2017 took different elevation as an aerial survey route to raise the image resolution which ranges between 0.036m to 0.190m, and 10 ground control points were set around the landslide area to calibrate the elevation. Moreover, Bentley Context Capture version 4.0 is used to feature the points of the aerial photos by aerotriangulation and produce the three-dimensional model, and the DSM grid size is 0.140m (Huang et al., 2017).

#### (2) Landslide simulation method

This study used the Integrated Rainfall-Infiltration Slope stability (IRIS) model to conduct the slope stability analysis. The IRIS model can be divided into several modules. The rainfall-infiltration module adopts the Richard's equation to simulate the infiltration and water flow in the soil. The result of infiltration analysis, which was calculated by the finite-element method, was then used to conduct a slope stability analysis simultaneously. A simplified Janbu method and dynamic programming (DP) method were used to determine the critical slip surface and the factor of safety (see **Fig. 2**).

According to the orthophoto and aspect map conducted by UAV after the disaster, the cross section of the landslide could be identified as the **Fig. 3**. The parameters used in the simulation were listed in **Fig. 4**, and they were obtained by filed survey and laboratory experiment. Therein, The lognormal model proposed by Kosugi(1996) can be used to represent  $C(\psi)$  and  $K(\psi)$  for unsaturated condition ( $\psi < 0$ ). The simulation used the rainfall data of Luye rainfall station from July 1 to September 13 as the antecedent rainfall, and prime simulation duration was from September 14 to September 15 with 10 minutes as the time-step of the simulation.

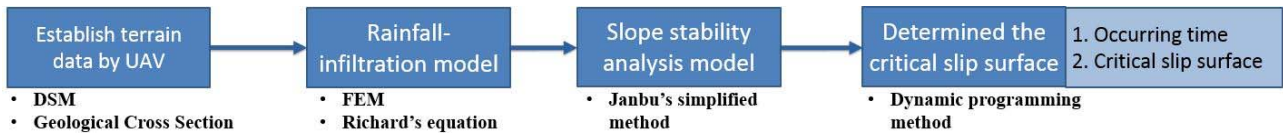


Fig. 2 The operating procedure of post-disaster survey and simulation.

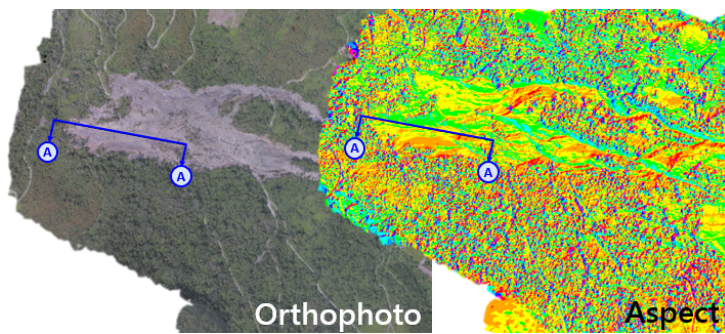


Fig. 3 Identify the cross section of landslide by orthophoto and aspect map

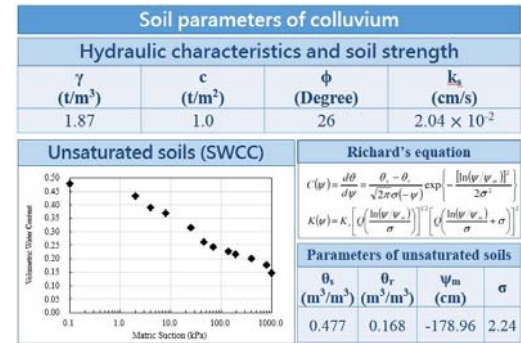


Fig. 4 Parameters of the simulation

### 3. RESULTS AND DISCUSSIONS

#### (1) Terrain change and volume evaluation

To compare the DSM before and after the landslide, the elevation difference after landslide and evaluates the landslide volume is determined. The results show that the landslide area is about 56,194 m<sup>2</sup>, and the mean elevation difference of the landslide area is 2.70 m, including the deepest erosion of 13.48 m and the highest accumulation of 21.25m (Fig. 5), and the landslide volume 211,466 m<sup>3</sup> is evaluated (Huang et al., 2017).

#### (2) Landslide simulation results

The simulation results show that the calculated slip surface from the simulation was very similar compared with the actual event (Fig. 6). Furthermore, the landslide occurring time of simulation is at 04:20 September 15 was also close to the actual disaster.

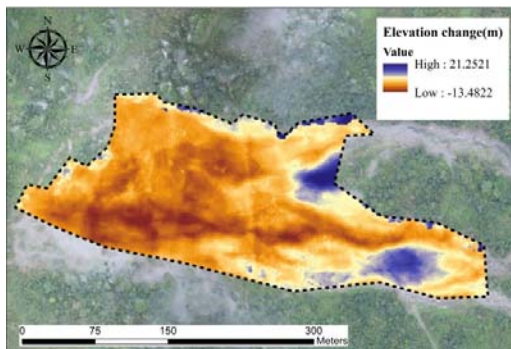


Fig. 5 Terrain change after landslide (Huang et al., 2017)

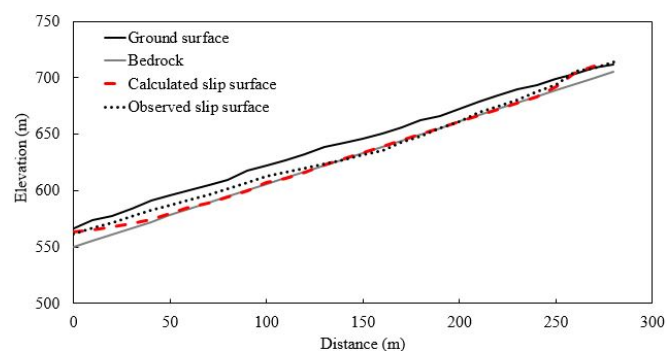


Fig. 6 The simulation results of landslide profile (A-A cross section)

### 4. CONCLUSIONS

UAV is an inexpensive, low-labor costs, effective, user-friendly and new remote-sensing tool, and it can quickly establish the orthophoto and DSM after post disaster. Applying the terrain data and soil parameters, IRIS model can simulate the scale and occurring time of landslide. To integrate these processes, this study establishes an operable standard operating procedure (SOP) for post-disaster survey and simulation for landslides. The SOP can help government officials to make appropriate decisions for post-disaster survey.

**Keywords:** Landslide, UAV, simulation, IRIS model, sediment disaster.

#### References

- 1) Feng-Chi Huang, Yi-Hsuan Lee, Jiun-Ting Lin, Kuo-Wei Chen, Chen-Yu Chen, Kuo-Lung Wang (2017): The Case Study for Evaluation of Landslides Volume and Moving Paths of Single Falling Rock, 5th GEDMAR.
- 2) Tsutsumi, D. and Fujita, M. (2008): Relative importance of slope material properties and timing of rainfall for the occurrence of landslides, International Journal of Erosion Control Engineering, Vol. 1, No. 2, pp. 79-89.
- 3) Kosugi, K. I. (1996): Lognormal distribution model for unsaturated soil hydraulic properties, Water Resource Research, Vol. 32, No. 9, pp. 2697-2703.